MECHANIKA TEORETYCZNA
I STOSOWANA
Journal of Theoretical
and Applied Mechanics
2, 34, 1996

FATIGUE CRACK BEHAVIOUR IN CARBURIZED AND LASER-HARDENED COMPONENTS MADE OF 18 HGM STEEL

STANISŁAW KOCAŃDA

LUCJAN ŚNIEŻEK

Department of Mechanical Engineering, Military University of Technology, Warsaw

Fatigue strength and fatigue crack behaviour in the carburized and laser-hardened 18HGM steel under reversed bending were studied. The structure, microhardness and residual stresses in the hardened zone were investigated. The Wöhler's diagram, the plots of crack length and crack growth rate versus numbers of cycles are presented in this paper. Characteristic features of a mechanism of crack initiation and propagation have been established on the basis of observations made under the SEM and TEM microscopes.

1. Introduction

Carburization and hardening are both generally known and accepted conventional means of case surface hardening of mating components. Great hardness of the hardened layer as well as high compressive residual stresses within this layer make the wear resistance higher and considerably increase fatigue strength of the structural members treated this way. Examination of fatigue behaviour of the laser hardened structural components has been carried out for many years in the Department of Mechanical Engineering of the Military University of Technology. The results obtained have suggested that conventional hardening of the carburized components can be replaced with the laser hardening. Fatigue testing of the components should follow. The results gained have become the contents of the publication presented and included into the series of earlier papers mentioned in the References hereafter. The paper has been aimed at investigating the fatigue crack behaviour within the carburized and laser-hardened specimens of the 18HGM steel with the fatigue

strength of the test pieces taken into account. Analyses of structures, as well as measurements of microhardness and residual stresses (all of them being necessary to give interpretation of the fatigue testing results) had been carried out prior to the investigations.

2. Experiment and results of investigations

Plane specimens made of the 18 HGM steel, 3.5 mm thick and of dimensions as in Fig.1., were examined.

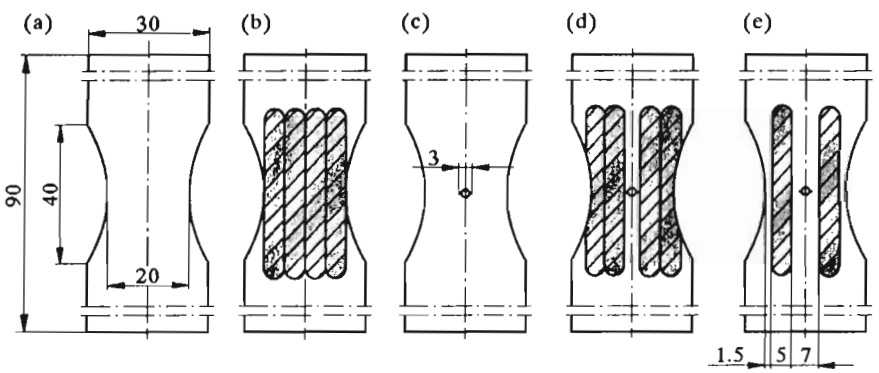

Fig. 1.

The grinded specimens were carburized in a solid medium at 900°C for 7 hours. Thickness of the carburized layer was 0.9 mm. Two lots of specimens had been prepared: conventionally and laser-hardened ones. Conventional treatment of the specimens consisted in oil quench hardening at temperature of 880°C followed by tempering at 190°C. The specimens of this lot served the purposes of comparative examination. The second, i.e., the due lot of test pieces included specimens hardened by a 1 kW CO_2 laser in nitrogen atmosphere at the laser beam rate 16.7 mm/s. The laser treatment was carried out at the Institute of Fundamental Technological Research of the Polish Academy of Sciences (IPPT PAN). The test pieces illustrated in Fig.1a and Fig.1b were intended for determining fatigue strength, whereas those in Fig.1c,d,e – for examining crack propagation and crack growth rates. The centrally positioned holes of 1.6 mm diameters were bored through the test pieces, all of them with slits 0.7 mm long on either side. Geometries and dimensions of

laser tracks (shaded areas) are shown in Fig.1b,d,e. The depth of the hardened track is equal to the depth of the carburized layer. The specimens were subjected to reversed bending of 25 Hz frequency.

Initiation and propagation of cracks were observed by means of a light microscope. Transmission and scanning electron microscopes (TEM and SEM, respectively) were used to examine fracture surfaces of the specimens. The research into fatigue properties of the specimens under investigation has been conducted at the considerable great contribution of P.Panek.

Structures of the specimens surface layer hardened in the conventional way were typical for thermo-chemical treatment of this kind. The structure of laser track at the specimen surface was formed of a regular martensitic structure that was changing towards the track bottom into a martensitic-bainitic structure and then into bainitic structure with ferrite precipitates. The observed images of the structures found expression in values and distributions of microhardnesses. Maximum microhardness of the conventionally hardened layer reached the level of $850\,\mu HV_1 00$, whereas of the laser-hardened one – $1000\,\mu HV_1 00$.

Values and distributions of the residual stresses can be mentioned among the most significant factors that have the influence on crack initiation and propagation in the laser-hardened components. The X-ray examination carried out with the $\sin^2\psi$ method showed the compressive residual stresses found on the total widths of the specimens. Residual stress measures have refered to the axial stresses normal to the track cross-section. The stresses mentioned reached the values of approximately 350 MPa within the laser tracks and 500 MPa in the zones between the tracks.

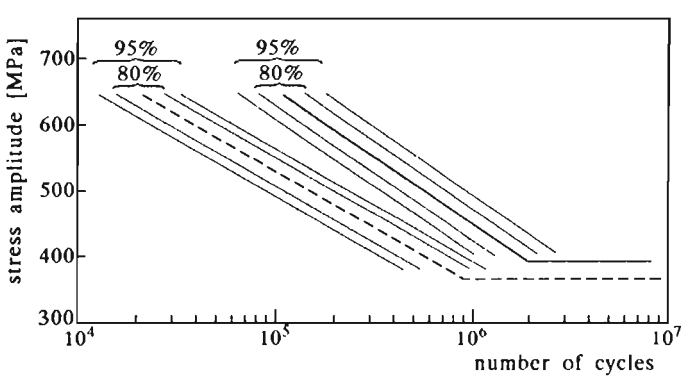

Fig. 2.

The results of fatigue strength testing have been presented in form of Wöhler's diagram (Fig.2). The diagram has been enriched with the confidence levels determined within the full range of loadings for the assumed probabilities of the specimen failure $P = 95\%$ and $P = 80\%$.

Little increase in fatigue strength has appeared at the simultaneously occurring well-marked increase in life within a range of limited fatigue strength of laser-hardened specimens (full line) as compared with the conventionally hardened ones (dashed line). The value of the fatigue limit has been accepted as equal to 390 MPa for the laser-hardened test pieces and to 370 MPa for the conventionally hardened specimens.

Determination in percentage of numbers of test pieces failured before reaching the pre-determined number of cycles is another form of visualizing the relationship between the stress amplitude σ_a and the number of loading cycles N. The proportion approximately determines probability P of failure specimens (Fig.3). Individual lines have been described with appropriate values of amplitude of stresses. The full lines represent the laser-hardened specimens, the dashed ones – the conventionally hardened test pieces. The beneficial effect of laser hardening, especially at lower values of the amplitude of stresses, has become evident.

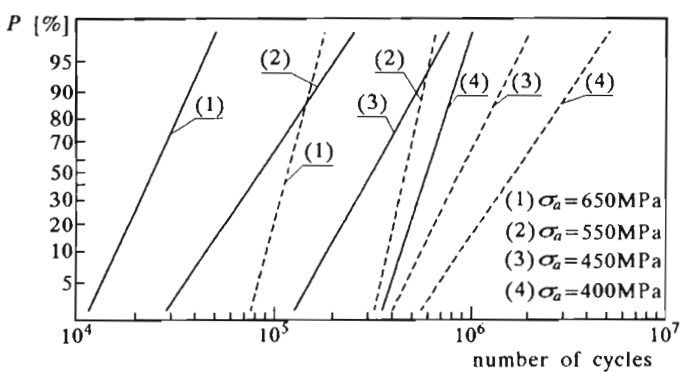

Fig. 3.

Crack propagation in the conventionally and laser-hardened specimens under examination was observed under reversed bending at stress amplitudes $\sigma_a = 300$, 350 and 400 MPa. The results of measurements taken have been plotted in the form of curves $l_i = f(N_i)$, where l_i current crack length measured from the tip of a slit after N_i cycles. An exemplary function $l = f(N)$ for the specimens with two tracks (shaded points) and four tracks (clear points) marked has been illustrated in Fig.4.

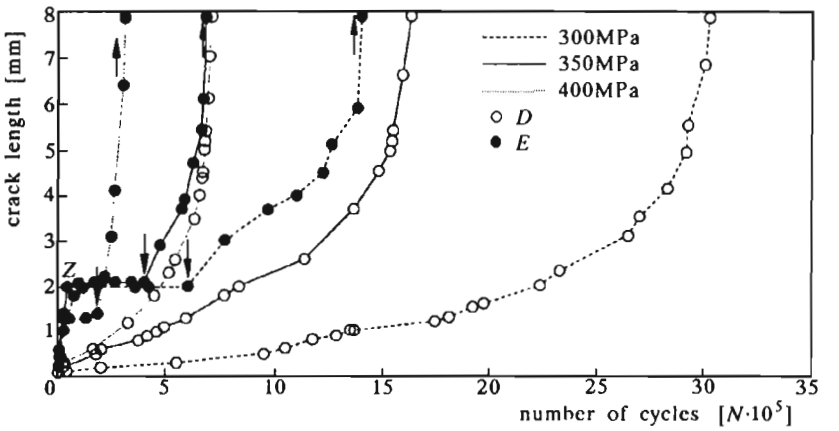

Fig. 4.

Characteristic feature of crack propagation in the specimens with two-track arrangements is periodic blocking of the fracture process at the border between the matrix material and the laser tracks. The crack blocking has been denoted with Z. Crack entrances into the tracks have been indicated with arrows showing downwards, whereas the exits – with arrowheads showing upwards. The periods of crack arresting were different depending on loadings imposed on the specimens and ranged from 10^5 cycles at $\sigma_a = 400\,\mathrm{MPa}$ to approximately $3 \cdot 10^5$ cycles at $\sigma_a = 300\,\mathrm{MPa}$. Regular increase in crack lengths on both ends of the slit was found to occur in the test pieces totally covered with osculating tracks. Rapid fracture of the conventionally hardened specimens made measuring the crack lengths impossible. Thus, there was no possibility to compare the results of examinning the test pieces after both types of hardening treatment. Measurements of crack lengths gave the grounds to calculate crack growth rates descibed with the Paris formula and related to the crack length 1, number of loading cycles N and the highest stress intensity factor $K_{\max}$. The exemplary plots of crack growth rates in Fig.5 refer to specimens with two tracks marked.

The zigzaggy fluctuations of crack growth rates have been affected by periodic retardation and accleration of crack propagation at the track and matrix borders and within the tracks themselves. The arrows show decreasing in crack growth rates down to the zero level, due to the above-mentioned periodical blocking at the track boundary. Owing to considerable irregularities of the plots affected it is nearly impossible to think of comparative analysis of crack growth rates in the individual, laser-hardened test pieces. Therefore, nothing

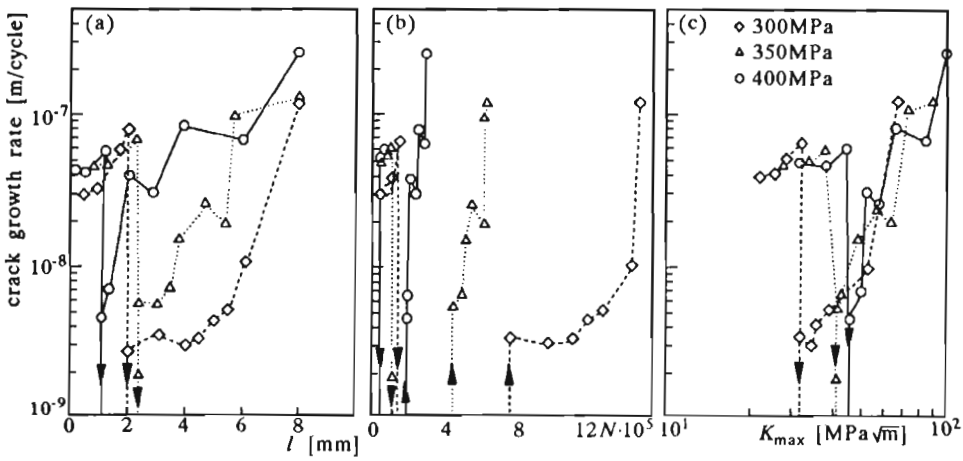

Fig. 5.

but general inference only seems to be feasible. No doubt the crack growth rate is considerably lower in the laser-hardened specimens than that in the conventionally treated ones, the efforts to measure the crack length increments in the latter ones having remained unsuccessful due to the rapid crack propagation. The crack was propagating most rapidly in the bands of matrix structures. In the course of crack propagation within the individual laser tracks the crack growth rate nearly equals to that in the test pieces with the whole surface hardened. Difficulties with comparing the failure processes and functions gained make us pay attention to better comparative measures given by diagrams of crack length increments depending on the number of loading cycles.

Observations of crack initiation and propagation (carried out within this work) have shown that in the specimens with the whole surface hardened the cracks were usually initiated in the spots where the tracks were in contact. The primary sources of cracks have been localized there. Fig.6 shows some examples of such sources of crack initiation. They illustrate the complexity of failure processes in laser-treated components and have been recognized as very interesting ones. The primary crack initiated in the above-mentioned regions between the tracks, being at the same time the regions of thermal influence on the tracks, propagates inside the test piece and under the track and seems to flow the track around (Fig.6b).

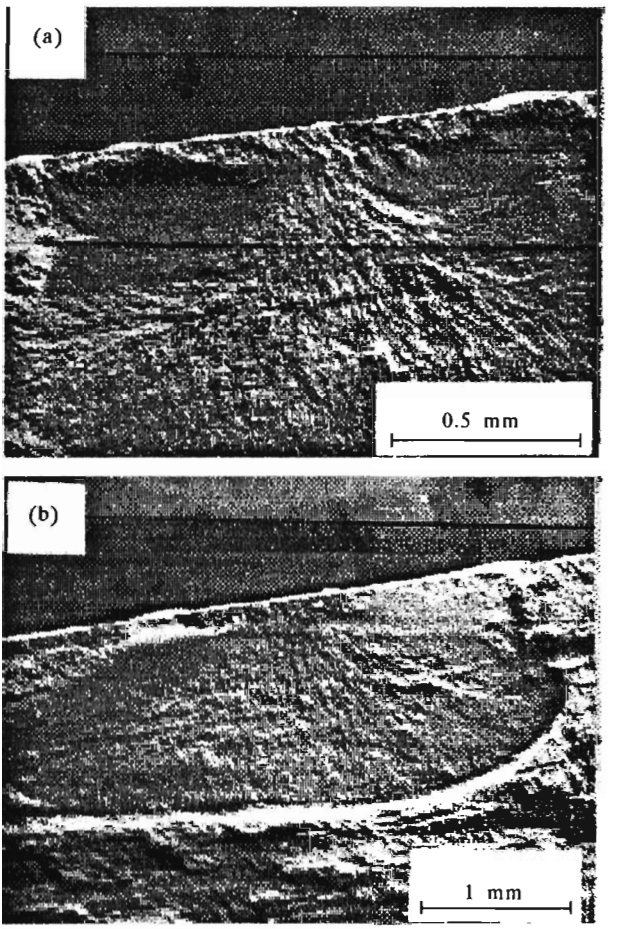

Fig. 6.

Micrographs taken with the transmission electron microscope (TEM) have shown the occurrences of cleavage fracture and brittle fractures along the grain boundaries (Fig.7a,b) within the near-surface laser-hardened layer. In the deeply located regions the share of cleavage fracture increases (Fig.7c,d). Crack *extending processes in the conventionally hardened test pieces were recognized* similar to those in the laser-hardened specimens. What was characteristic of them was considerably greater violency of crack growth resulting in much greater share of cleavage fracture.

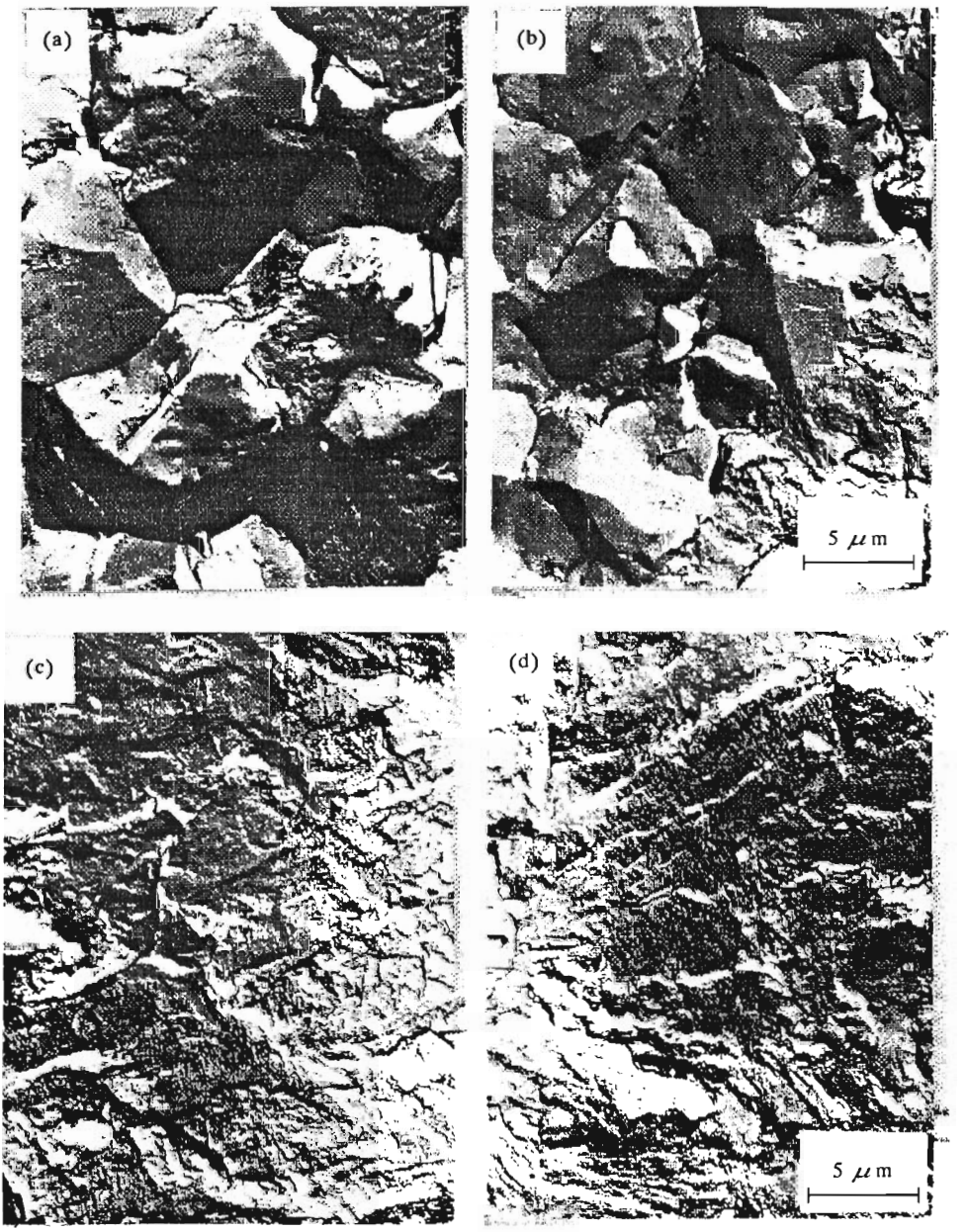

Fig. 7.

3. Final remarks

The carburized and laser-hardened components made of the 18HGM steel have shown better fatigue properties under reversed bending conditions as compared to properties of similar components, conventionally hardened, however. Fatigue strength increases three times at $\sigma_a = 400$ MPa and four times at $\sigma_a = 600$ MPa as compared with fatigue strength of conventionally hardened specimens. Only slightly, i.e., by not more than a few percent the fatigue limit has increased. Propagation of fatigue cracks and crack growth rate seems to take advantageous orientation. Failure processes are significantly delayed in the laser-hardened test pieces as compared to the rapid crack growth phenomena found in the conventionally hardened specimens. The feature is of considerable importance in the case cracks initiate. It is closely related to the structures, residual stresses and geometry of the laser-hardened tracks. These, in turn, are strongly influenced by the conditions of laser treatment. Examination of fracture microstructures made by the TEM has enabled primary and secondary sources of crack initiation to be localized, as well as complexity of the mechanism of fracture to be thoroughly studied. While propagating from the specimen surface down into its depth the nature of fracture was changing from the mixed brittle fracture along the grain boundaries and cleavage fracture through to the quasi-cleavage fracture with plastic deformation symptoms noted.

Results of examining the carburized and laser-hardened test pieces made of the 18HGM steel should be recognized as guidelines to subsequent tests of specific machine components such as gears, necks of various types of shafts, etc.

The authors gratefully acknowledge support of the State Committee of Scientific Research under grant No 7S10107604.

References

1. KOCAŃDA S., NATKANIEC D., 1992, Fatigue Crack Initiation and Propagation in Laser Hardened, Medium Carbon Steel, *Fatigue Fract. Engng Mat. Struct.*, **15**, 12, 1237-1249

2. KOCAŃDA S., NATKANIEC D., ŚNIEŻEK L., 1994, Fatigue Behaviour of Laser Hardened Steels – Comparison Study of Low, Medium Carbon Steel, High Strength and Carborized CrMn Steels, Localized Damage'94, Third Int. Conf.

Udine, Italy, *Computational Mechanics Publications*, Southhampton - Boston, 29-37.

3. KOCAŃDA S., PANEK P., ŚNIEŻEK L., 1993, Wlasności zmęczeniowe nawęglanych i laserowo hartowanych elementów ze stali 18HGM, (in Polish), *Biul. WAT*, **4**, 3-22
4. KOCAŃDA S., ŚNIEŻEK L., 1993, Zmęczeniowe pękanie laserowo wzmocnionych elementów ze stali o podwyższonej wytrzymalości 18G2, (in Polish), *Letters of Świętokrzyska Polytechnik, Mechanika*, **50**, 251-258
5. NATKANIEC D., KOCAŃDA S., MILLER K.J., 1994, Short Fatigue Crack Growth in Laser Hardened Medium Carbon Steel, *J. Theoret. and Appl. Mechanics*, **32**, 1, 163-176

Powstawanie i rozwój pęknięć zmęczeniowych w nawęglanych i laserowo hartowanych elementach ze stali 18HGM

Streszczenie

Zbadano własności zmęczeniowe nawęglanych i laserowo hartowanych elementów modelowych ze stali 18HGM. Omówiono strukturę, mikrotwardość i naprężenia własne w warstwie zahartowanej. Wykonano wykresy Wöhlera. Zlokalizowano źródla pęknięć i obserwowano rozwój pękania. Podano wykresy przyrostu dlugości pęknięć oraz wykresy prędkości pękania w zależności od długości pęknięć, liczby cykli obciążenia i współczynnika intensywności naprężeń. Na podstawie elektronooptycznych badań mikrobudowy powierzchni pęknięć opisano mechanizm pękania. Własności zmęczeniowe nawęglanych i laserowo hartowanych elementów okazały się istotnie lepsze od własności konwencjonalnie nawęglanych i hartowanych elementów.

Manuscript received December 5, 1995; accepted for print December 18, 1995